

Effects of gamma radiation on optical fibre sensors

K.-C. Lin, C.-J. Lin and W.-Y. Lee

Abstract: Consideration of thermo-optic coefficients is essential in the applications of optical fibre sensors and high-speed fibre communication systems. The Fabry–Perot interference method is applied to study these coefficients of four types of commercial fibres. The results are in agreement with the values calculated from the Sellmeier equation for fused silica fibre, with a difference of only about 0.2% for the Corning single-mode fibre SMF-28. In order to apply fibre sensors to a high-radiation environment, the thermo-optic coefficients for these fibres have been investigated after exposure to heavy doses of gamma radiation, and their radiation resistance has been studied.

1 Introduction

Fibre optic technology has recently been considered for applications in harsh gamma radiation environments, for example, in nuclear power plants [1, 2]. In particular, the effects of gamma radiation on the transmission characteristics of optical fibres have been extensively studied [2]. Because silica glass (SiO_2) is a basic optical fibre material, it has been extensively used to make various kinds of optical fibres, amplifiers [3], and fibre lasers [4] with suitable doping materials since the late 1960s. The refractive index and its variation as a function of temperature, i.e. the thermo-optic coefficient dn/dT , are important characteristics of silica-based glasses, which are necessary for the evaluation of optical fibre transmission system designs using such glass optical fibres. In particular, the change of the fibre thermo-optic coefficient after the fibres have been exposed to gamma radiation is a major factor for fibre communication and fibre sensors used in a nuclear power plant. In general, the thermo-optic coefficients are measured at discrete wavelengths in the transmission range of the glasses [5]. Fibre Bragg grating-based sensors, with high accuracy of the thermo-optic coefficient ($<3\%$), under irradiation up to very high doses ($>1\text{Mgy}$) have been reported [1]. In this work, we propose a novel method that uses a fibre Fabry–Perot etalon to understand the relationship between the refractive index and temperature for a glass fibre. There is excellent agreement between our research results and the results derived by adopting the Sellmeier equation [6]. Then, we irradiated four different commercially available optical fibres with three different gamma-ray doses to investigate the temperature sensitivity of the fibre under high-dose radiation.

2 Theoretical design and fabrication

When light is guided into a fibre Fabry–Perot interferometric (FFPI) sensor [7], as shown in Fig. 1, a portion of the light reflected from each internal reflector generates an interference effect. The interference is created constructively (i.e. reflections are in phase with each other) or destructively (i.e. reflections are out of phase with each other). The measured phase shift is a result of changes in the refractive index and/or changes in the length of the sensor cavity with respect to the wavelength of light. The relation of the optical phase shift is $\Delta\phi = 4\pi\Delta(nL)/\lambda$, where n is the refractive index of the fibre, L the length of the sensor cavity, and λ the wavelength of the laser light [8]. If the sensor is exposed to thermal variations, the phase change of the sensor is [9]

$$\Delta\phi = 2kL\left(\frac{dn}{dT}(\rho) + \frac{n}{L}\frac{dL}{dT}\right)\Delta T \quad (1)$$

where k is the wavenumber, $(1/L)(dL/dT)$ is the thermal expansion coefficient ($\simeq 5.5 \times 10^{-7}/^\circ\text{C}$ for silica fibre), and dn/dT is the thermo-optic coefficient (typically $1 \times 10^{-5}/^\circ\text{C}$ for silica fibre without gamma irradiation). Two major mechanisms, the change in the refractive index and that in the physical length, affect the phase shift. Because the value of dn/dT is 20 times greater than that of $(1/L) \times (dL/dT)$, the sensitivity of the FFPI sensor is dominated by the index change. Also, the sensitivity of the sensor increases with longer sensor cavity and shorter wavelength source. As will be shown in Section 4, there are linear relations between the thermo-optic coefficient and the gamma-irradiation doses (ρ). The linear radiation-dependence coefficient is referred to as κ ($10^{-5}/^\circ\text{C}/\text{kGy}$). Therefore, (1) can be reformulated to be

$$\Delta\phi = 2kL\left(\kappa \cdot \rho + \frac{n}{L}\frac{dL}{dT}\right)\Delta T \quad (2)$$

Depending on the amount of the refractive index change or the change in the sensor cavity length due to perturbation, the reflective power will sweep through maximum and minimum interference effects. These signals can be processed to determine the amount of perturbation; in addition, they allow one to obtain an accurate thermo-optic coefficient value with respect to the fibre sensor.

The experimental arrangement for testing the FFPI temperature sensor is illustrated in Fig. 2. The supported

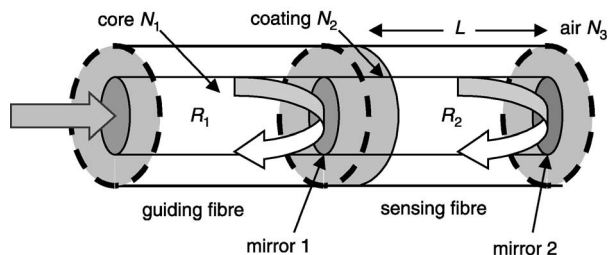


Fig. 1 Schematic illustration of the Fabry-Perot optical fibre sensor

photoelectronics comprises a DFB laser diode with an operating centre wavelength at 1553.9 nm and a very narrow linewidth ($\Delta\lambda \approx 2$ MHz), an InGaAs photodetector, and a 2×2 fused biconical tapered coupler which delivers light to and from the sensor head. The laser light is guided into a Faraday isolator which eliminates feedback from the fibre into the laser, before the fibre pigtail is connected with a 2×2 directional coupler. An InGaAs photodetector is used to detect the reflected optical power and is connected with a power meter (HP-34401A) to measure the output voltage. A K-type thermocouple, which detects the temperature in the oven and serves as a reference instrument, is also connected with the power meter (HP-3478A). The fibre sensor and the reference thermocouple are put in the oven together. A precision temperature controller is used to control the oven temperature. We use PID (proportional band, integral time and derivative time) process programs to set up the temperature increment rate at 0.5°C per minute. All experiments are performed inside a clean room with stable temperature and humidity. Automation of the experiment can greatly increase the accuracy of the data acquisition. We set up an automatic data-acquisition system composed of a personal computer, an ANSI/IEEE-488.2 (GPIB) system, and the Lab-Windows software. The measurement system can record the photodetector output voltages, the reference thermocouple output voltages, and the lock-in amplifier output intensities and phase differences.

3 Results and discussion

The response of the FFPI sensor made from the Corning SMF-28 fibre with cavity length 2.42 mm is shown in Fig. 3. The stars represent the output light intensity received by the photodetector. As illustrated, the output signal oscillates

periodically with the temperature and the period of the oscillation remains constant within the temperature range from 30°C to 180°C . The oscillation period is found to be 31.27°C . The solid line shows the theoretical result. In this theoretical simulation, it is assumed that the first mirror reflectance is $R_1 = 0.06$, the second mirror reflectance is $R_2 = 0.06$; the wavelength of the DFB laser is $\lambda = 1553.9$ nm, and the thermo-optic coefficient is $dn/dT \approx 1.06323 \times 10^{-5}$. The FFPI sensor induces a phase change of 2π in each temperature period, which satisfies (2). The phase changes plotted in Fig. 4 are determined by counting the fringes. The solid line in this Figure represents a linear fit to the counted data. There are about eight fringes from 30°C to 250°C in this case, and the results from the experiment are a function of the temperature which is measured with the thermocouple. To calculate the thermo-optic coefficient, the Sellmeier method is the best formula because of its sound physical basis [6]. The two-pole Sellmeier formula is a physically meaningful model to represent the refractive index as a function of wavelength. One pole arises from electric resonance absorption, and the other stems from lattice/ionic resonance absorption.

The wavelength-dependent Sellmeier equation is of the form [10]:

$$n^2 = A + \frac{B}{\left(1 - \frac{C}{\lambda^2}\right)} + \frac{D}{\left(1 - \frac{E}{\lambda^2}\right)} \quad (3)$$

where λ is the wavelength in μm . The first and second terms represent, respectively, the contribution to the refractive indices due to higher and lower energy gaps of electronic absorption. The Sellmeier coefficients of fused silica (SiO_2) are $A = (6.90754 \times 10^{-6})T + 1.31552$, $B = (2.35835 \times 10^{-5})T + 0.788404$, $C = (5.84758 \times 10^{-7})T + 0.0110199$, $D = (5.48368 \times 10^{-7})T + 0.91316$, and $E = 100$ [6], where T is the temperature in degrees centigrade.

For the fused silica fibre, the calculated thermo-optic coefficient dn/dT is about $1.062221 \times 10^{-5}/^\circ\text{C}$. For the Corning single-mode fibre SMF-28, a type of fused silica fibre, its experimental thermo-optic coefficient value dn/dT is $1.06323 \times 10^{-5}/^\circ\text{C}$, which is very close to the result calculated from the Sellmeier equation, and the inaccuracy ratio between the calculated and experimental result is about 0.2%.

In the experiment, we used four kinds of commercially available fibres: Corning SMF-28, the 3M single-mode fibre

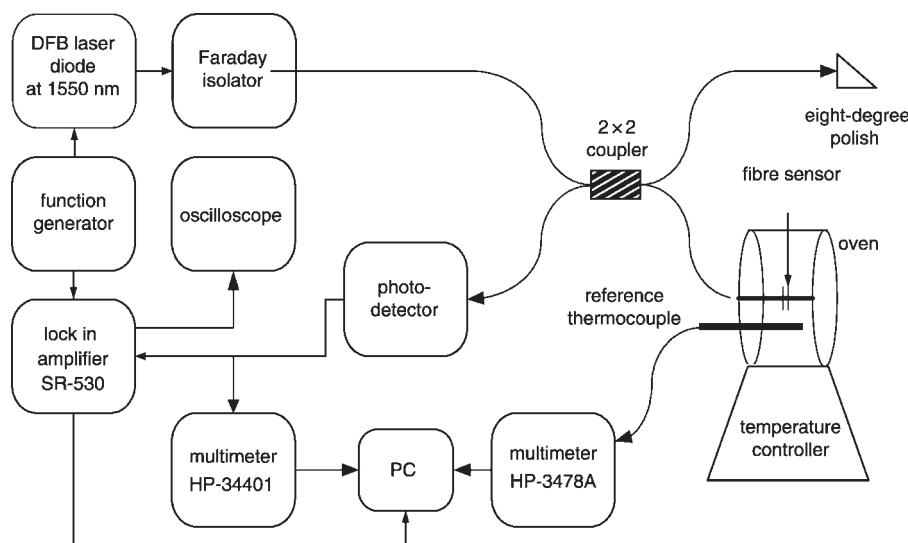


Fig. 2 Experimental set-up to measure the FFPI temperature sensor

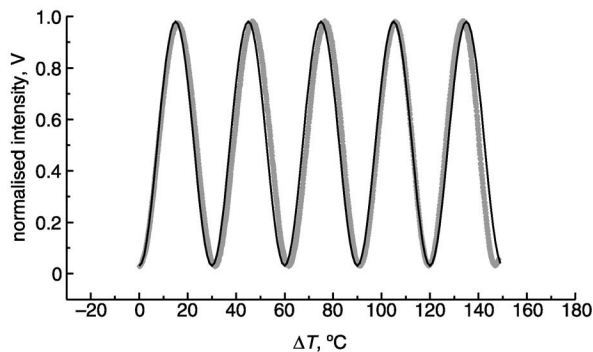


Fig. 3 Normalised temperature response of the FFPI sensor (Corning SMF-28 fibre)

The stars denote experiment results and the solid line denotes theoretically simulated results

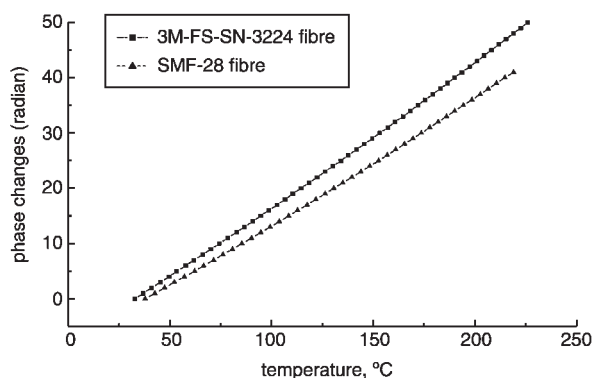


Fig. 4 Temperature dependence of the measured phase changes of the FFPIs for two better-quality fibres, SMF-28 and FS-SN-3224. Experimental results and their linear fits are shown

FS-SN-3224, POFC fibre PHOCLD-15, and Suprail fibre F-110, to make the FFPI fibre sensor. They all have excellent intensity responses and linear phase changes for temperatures from 30°C to 250°C and their experimental thermo-optic coefficient values are shown in Table 1. Also in Fig. 4, the temperature dependence of the measured phase changes for two better-quality fibres, SMF-28 and FS-SN-3224, is shown for comparison.

We compare the gamma radiation responses of four different types of commercially available optical fibres by measuring their thermo-optic coefficient values. Figure 5

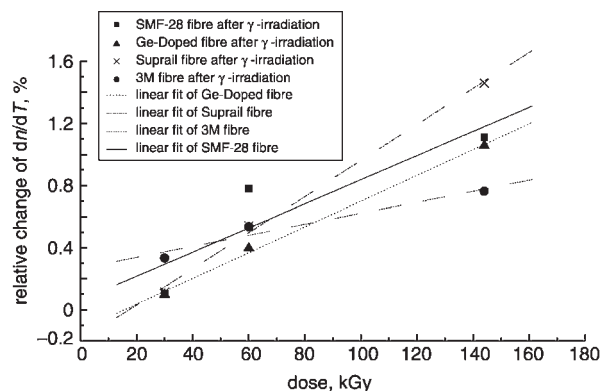


Fig. 5 Thermo-optic coefficient variations of four different commercial fibres after high doses of gamma irradiation

shows the thermo-optic coefficient variations of the four different commercial fibres after high doses of gamma irradiation. Each time we made four kinds of FFPI fibre sensors with the different fibre materials. Initially, we measured the responses of the FFPI fibre sensors from 30°C to 250°C, and calculated the thermo-optic coefficients dn/dT before gamma-ray exposure. Next, the FFPI fibre sensors were subjected to three successive gamma-ray exposures using a ^{60}Co source at a dose rate of 5 kGy per hour for 6 hours, 12 hours, and 28.8 hours, and the irradiation temperature was about 35°C. The total increment doses were 30 kGy, 60 kGy and 144 kGy. We measured the responses of the irradiated FFPI fibre sensors in the same temperature range and computed the thermo-optic coefficients for all sensors. We discovered that the alterations of the fibre sensors bear a closely linear relation to different doses of gamma irradiation. However, the change of the thermo-optic coefficient value yields incorrect temperature measurement results and the analysis system should always be calibrated when the alternation happens. For example, in outer space or inside nuclear power plants, the low radiation resistance of optical fibres is unacceptable for optical electronic systems intended for use in harsh radiation environments.

As shown in Fig. 5, the solid points represent changes in the thermo-optic coefficient value of the Corning SMF-28 fibre sensor after gamma irradiation. The alterations are 0.105% for 30 kGy dose, 0.783% for 60 kGy dose, and 1.112% for 144 kGy dose. The other results, including the stars representing Ge-doped fibre (POFC fibre PHOCLD15), the circles representing Suprail fibre F-110

Table 1: Experimental thermo-optic coefficients of several fibres

Fibre category	Corning fibre (SMF-28)	POFC fibre (PHOCLD15)	Suprail fibre (F-110)	3M fibre (FS-SN-3224)
$(dn/dT) \times 10^{-5}$	1.06323	1.05202	1.03181	1.03046

Table 2: Thermo-optic coefficient increase after gamma irradiation

	Corning fibre SMF-28	POFC fibre PHOCLD15	Suprail fibre F-110	3M fibre FS-SN-3224
$(dn/dT) \times 10^{-5}$ before dose	1.06323	1.05202	1.03181	1.03046
Dose 30 kGy	0.105%	0.098%	0.114%	0.333%
Dose 60 kGy	0.783%	0.396%	0.542%	0.536%
Dose 144 kGy	1.112%	1.057%	1.46%	0.763%

and squares representing 3M SMF FS-SN-3224 also show an increase with incremental radiation doses. The data are listed in Table 2.

The 3M SMF FS-SN-3224 has the best radiation resistance and the lowest variation in thermo-optic coefficient. The Corning SMF-28 fibre and POFC fibre PHOCLD15 have similar responses in regard to the differences of the thermo-optic coefficients. Suprail fibre F-110 is the worst fibre in the gamma radiation environment as manifested by its acute change. We suggest that a fibre sensor made of Suprail fibre F-110 is not a very practical temperature gauge in nuclear power plants. Furthermore, to apply FFPIs to nuclear power plants as remote temperature monitors, the radiation resistance of fibre-optic sensors can be improved by using F-doped fibres, and the temperature distribution can be correctly measured by the loop-arrangement calibration technique [11].

4 Conclusions

Instrumentation and control systems are vital for safety of nuclear plant. With a view to applying a fibre sensor in a harsh radiation environment, the effects of high radiation doses on optical fibres have been studied in this paper. By analysing the results of all the fibre temperature sensors in the experiment, we have obtained four kinds of thermo-optic coefficient value for commercially available optical fibres. The value, for example, of the Corning SMF-28 fibre is in excellent agreement with that calculated by using the Sellmeier equation for fused silica fibre. The difference rate is about 0.2%. Using our measurement system, we not only easily obtain the thermo-optic coefficient values of fibres but also find that the thermo-optic coefficient value is approximately linearly related to increasing gamma radiation doses. Among the four kinds of fibres in this experiment, 3M SMF FS-SN-3224 is the best choice for fibre sensors used in the gamma radiation environment. Moreover, several specific optical fibres with novel materials have been presented [11] for fibre sensors to be

applied as thermo-monitors in harsh radiation environments. The results demonstrated in this paper would be a good basis for further research and applications in fibre sensors or nuclear science.

5 Acknowledgments

The authors would like to thank the National Nuclear Research Council and Wistek Tech Ltd. for experimental support. This work was funded by the National Science Council of the Republic of China under contracts NSC92-2622-E-229-001 and NSC92-2215-E-229-001.

6 References

- 1 Gusarov, A.I., Berghmans, F., Deparis, O., Fernandez, A., Defosse, Y., Megret, P., Decreton, M., and Blondel, M.: 'High total dose radiation effects on temperature sensing fiber Bragg gratings', *IEEE Photonics Technol. Lett.*, 1999, **11**, pp. 1159–1161
- 2 Berghmans, F., Vos, F., and Decreton, M.: 'Evaluation of three different optical fiber temperature sensor types for application in gamma radiation environments', *IEEE Trans. Nucl. Sci.*, 1998, **45**, pp. 1537–1542
- 3 Li, T.: 'Fiber fabrication, optical communication' (Academic Press, New York, USA, 1985), vol. 1
- 4 Takahashi, Y., and Yoshino, T.: 'Fiber ring laser with flint glass fiber and its sensor applications', *J. Lightwave Technol.*, 1999, **17**, pp. 591–597
- 5 Samanta, L.K., Ghosh, G.C., and Bhar, G.C.: 'Temperature dependence of refractive indices in some nonlinear crystals', *Indian J. Phys.*, 1980, **54B**, pp. 426–434
- 6 Ghosh, G., Endo, M., and Iwasaki, T.: 'Temperature-dependent Sellmeier coefficients and chromatic dispersions for some optical fiber glasses', *J. Lightwave Technol.*, 1994, **12**, pp. 1338–1342
- 7 Lee, C.E., and Taylor, H.F.: 'Interferometric optical fiber sensors using internal mirrors', *Electron. Lett.*, 1988, **24**, pp. 193–194
- 8 Lee, C.E., Taylor, H.F., Markus, A.M., and Udd, E.: 'Optical-fiber Fabry-Perot embedded sensor', *Opt. Lett.*, 1989, **14**, pp. 1225–1227
- 9 Lee, C.E., Atkins, R.A., and Taylor, H.F.: 'Performance of a fiber-optic temperature sensor from –200 to 1050°C', *Opt. Lett.*, 1988, **13**, pp. 1038–1040
- 10 Ghosh, G.: 'Sellmeier coefficients and dispersion of thermo-optic coefficients for some optical glasses', *Appl. Opt.*, 1997, **36**, pp. 1540–1546
- 11 Kimura, A., Takada, E., Fujita, K., Nakazawa, M., Takahashi, H., and Ichige, S.: 'Application of a Raman distributed temperature sensor to the experimental fast reactor JOYO with correction techniques', *Meas. Sci. Technol.*, 2001, **12**, pp. 966–973